

# Selection of Protein–Protein Interactions of Desired Affinities with a Bandpass Circuit

Katherine E. Brechun<sup>1,2</sup>, Katja M. Arndt<sup>2</sup> and G. Andrew Woolley<sup>1</sup>

**1** - Department of Chemistry, University of Toronto, Toronto, Canada

**2** - Molecular Biotechnology, University of Potsdam, Potsdam, Germany

**Correspondence to Katja M. Arndt and G. Andrew Woolley:** [katja.arndt@uni-potsdam.de](mailto:katja.arndt@uni-potsdam.de), [awoolley@chem.utoronto.ca](mailto:awoolley@chem.utoronto.ca)  
<https://doi.org/10.1016/j.jmb.2018.11.011>

**Edited by Amy Keating**

## Abstract

We have developed a genetic circuit in *Escherichia coli* that can be used to select for protein–protein interactions of different strengths by changing antibiotic concentrations in the media. The genetic circuit links protein–protein interaction strength to  $\beta$ -lactamase activity while simultaneously imposing tuneable positive and negative selection pressure for  $\beta$ -lactamase activity. Cells only survive if they express interacting proteins with affinities that fall within set high- and low-pass thresholds; i.e. the circuit therefore acts as a bandpass filter for protein–protein interactions. We show that the circuit can be used to recover protein–protein interactions of desired affinity from a mixed population with a range of affinities. The circuit can also be used to select for inhibitors of protein–protein interactions of defined strength.

© 2018 Elsevier Ltd. All rights reserved.

## Introduction

Protein–protein interactions are fundamental mediators of biological processes ranging from gene expression to immune responses [1]. In numerous cases, it has been observed that, to be functional, a protein–protein interaction should be neither too weak nor too tight, but just right (this observation has been termed the Goldilocks principle [2,3]). For example, several studies have found that when the affinity of a peptide/major histocompatibility complex for a T-cell receptor is either too low or too high, immune responses can be impaired [3,4]. Likewise, basic leucine zipper (bZIP) transcription factors homo- and heterodimerize with a range of affinities leading to complex interaction profiles, thereby controlling gene expression with massive combinatorial regulatory potential [5]. Because binding affinities set bounds on binding and dissociation rates, precisely tuned binding affinities are important for the dynamic interplay of protein partners and temporal responsiveness to changes in the environment [6,7]. Perturbation of finely balanced protein–protein interactions is central to numerous diseased states [8,9].

An ability to develop new protein–protein interactions and modify existing ones is foundational for numerous

applications in biotechnology and medicine. For example, moderate-affinity, rather than high-affinity, T-cell receptor interactions have been proposed to be less likely to lead to unwanted toxic responses in T-cell-based immunotherapies [3,10]. Likewise, protein-based drug delivery systems require tuning of carrier protein affinity in order to control drug release rates and achieve a desired *in vivo* release profile [11]. Systems that enable selection of a specific level of activity may also be used to evolve switchable proteins by changing the target level of activity in response to a given set of external cues [12].

Current approaches for *in vivo* selection of interacting protein partners focus on the recovery of interactions with maximal binding strength, eliminating interactions below a selection threshold [13,14]. Selection methods for discovering and developing protein–protein interactions do uncover interactions of different affinity during the course of a multiple-round selection by varying (or relaxing) stringency, and it has been observed that yeast two-hybrid (Y2H) studies show some correlation between growth rates and protein–protein interaction affinity [14]. Also, by reprogramming sexual agglutination of yeast to allow library on library screening for protein–protein interactions, Younger *et al.* [15] showed that next-generation sequencing of the resulting diploid

yeast strains could allow for quantitative evaluation of thousands of pairwise interactions. While these methods do link growth to the strength of a protein-protein interaction, they do not offer a way of specifically selecting for an intermediate affinity while avoiding higher-affinity clones. Using yeast surface display together with a defined binding target, a library of binding partners can be sorted using flow cytometry [16]. Reich and colleagues [17] have used this approach together with next-generation sequencing to rank hundreds of yeast-displayed peptides according to their affinities for a target protein. In this manner, strong, medium and weak affinity binders can be recovered, however, because it is a screening system rather than a selection system, this approach is more limited in the numbers of variants that can be assayed.

Here, we introduce a genetic circuit in *Escherichia coli* that can act as a bandpass filter for protein-protein interactions and show, using proof-of-principle test

cases, that the circuit allows one to select for protein-protein interactions of different strengths by changing the antibiotic concentrations in the media. To create this system, we combined two previously established sub-circuits: a hitchhiker circuit that links protein-protein interaction strength to  $\beta$ -lactamase activity [18,19], and a bacterial bandpass filter that allows for selection for cells with specific, tunable levels of  $\beta$ -lactamase activity [12] (Fig. 1). The hitchhiker circuit uses the endogenous twin-arginine translocation (Tat) pathway, a bacterial export system across the cytoplasmic membrane that accepts only folded substrates [21,22], to select for interacting proteins. It has been shown previously that a protein lacking a signal sequence can be transported to the periplasmic space *via* the Tat pathway by interacting with a protein bearing a Tat-targeting signal sequence—a process termed “hitchhiking” [21–23]. The hitchhiker circuit uses this process to detect protein-protein interactions by fusing one half of an

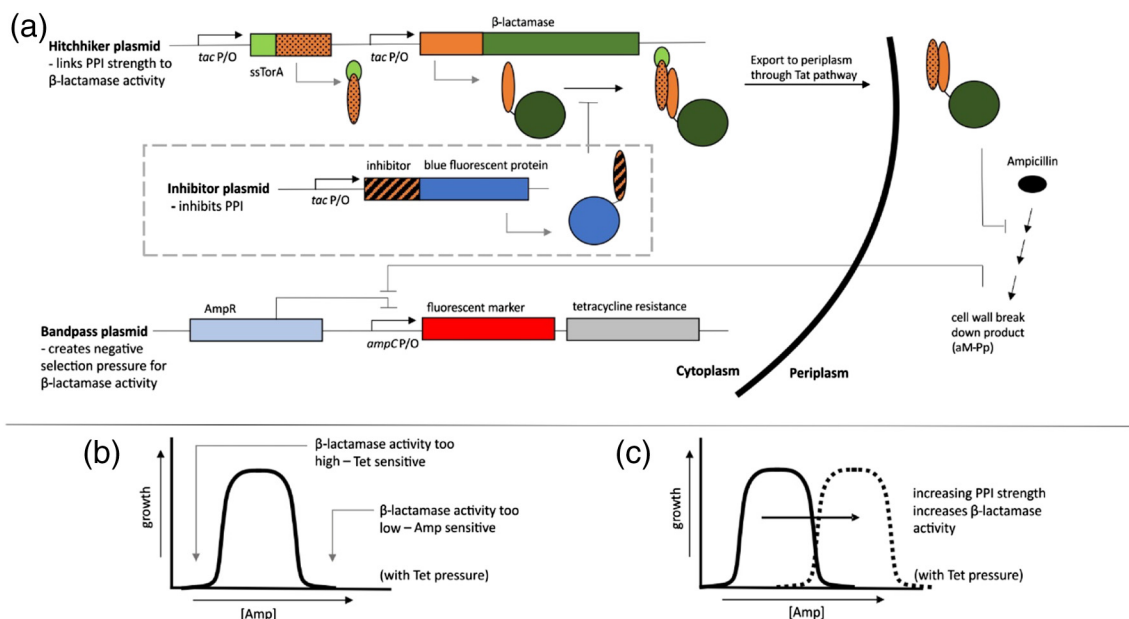


**Fig. 1.** (a) Selection of protein-protein interactions of desired affinities with a bandpass circuit. The hitchhiker plasmid (top) creates a circuit linking protein-protein interaction strength to cellular Amp resistance levels. When the two hitchhiker constructs interact (orange dotted and solid orange), a complex is formed that non-covalently links the Tat-targeting signal sequence (light green) to a  $\beta$ -lactamase devoid of its native signal sequence (dark green). This protein-protein interaction allows the  $\beta$ -lactamase to “hitchhike” to the periplasm *via* the Tat transport pathway where it hydrolyzes Amp (black oval). Co-expression of an inhibitor (orange stripes) targeting the hitchhiker pair impedes hitchhiker complex formation, lowering cellular Amp resistance levels. This component is optional (dashed box) and is discussed in the second half of the paper. The bandpass plasmid (bottom) produces a circuit that leads to negative selection pressure for  $\beta$ -lactamase activity in the presence of Tet. The plasmid encodes a gene for Tet resistance that is under the control of the *ampC* promoter, which is constitutively repressed by the AmpR transcriptional regulator. When bound by the cell wall breakdown product aM-Pp, AmpR becomes an activator for the *ampC* promoter [20]. (b) The combined positive and negative selection pressure for  $\beta$ -lactamase activity limits cell growth to a specific range of Amp concentrations. High concentrations of Amp prevent growth because the  $\beta$ -lactamase activity is insufficient. Low concentrations of Amp prevent growth because the  $\beta$ -lactamase activity is too high; there is no cell wall damage and the Tet resistance gene is not expressed (*i.e.*, cells are Tet sensitive). At intermediate concentrations of Amp, the  $\beta$ -lactamase activity balances the Amp concentration, such that cells survive the pressure, yet sustain non-lethal cell wall damage, leading to expression of the Tet resistance gene. (c) The Amp concentration permitting growth is dictated by the  $\beta$ -lactamase activity level, which is linked to PPI strength. Increasing the PPI strength therefore changes the concentration of Amp permitting growth.

interacting protein pair to a Tat-targeting signal sequence, and the second half to a selectable marker, namely,  $\beta$ -lactamase devoid of its native signal sequence.  $\beta$ -Lactamase hydrolyzes  $\beta$ -lactam antibiotics, such as ampicillin (Amp), protecting bacteria from cell wall damage [24]. To fulfill this role,  $\beta$ -lactamase must be transported to the periplasm. While several factors may influence the  $\beta$ -lactamase activity observed, including Tat-transport efficiency and protein expression levels, the interaction strength of the pair of hitchhiker proteins has been shown to be a dominant factor for controlling the amount of  $\beta$ -lactamase transported and thereby for controlling cellular Amp resistance levels [19]. We expand on the hitchhiker translocation system by incorporating an inhibitor targeting the hitchhiker pair (Fig. 1, inset). We show the binding strength of the inhibitor is inversely correlated with the cellular Amp resistance levels.

The hitchhiker circuit, with or without an inhibitor, achieves the high-pass component of the bandpass filter by allowing for cell growth only when cellular  $\beta$ -lactamase activity is high enough to counteract the growth inhibitory effect of Amp. To complete the bandpass filter, cells are simultaneously subjected to negative selection pressure for  $\beta$ -lactamase; that is, cells with  $\beta$ -lactamase activity above a certain level also do not survive. This is achieved by co-opting an endogenous transcriptional response to  $\beta$ -lactam antibiotics present in nearly all members of the *Enterobacteriaceae* family [24]. The presence of a  $\beta$ -lactam antibiotic leads to accumulation of cell wall breakdown products, which are imported into the cytoplasm and metabolized as part of the peptidoglycan recycling pathway [24]. One of the resulting fragments, 1,6-anhydroMurNAc-pentapeptide (aM-Pp), has been shown to bind to the transcriptional regulator AmpR, leading to the transcription of a genomic  $\beta$ -lactamase (AmpC) via the *ampC* promoter [25]. In the present work, the *ampC* promoter and AmpR from *Citrobacter freundii* [26] are used to control the production of a tetracycline (Tet) resistance gene, as well as a fluorescent marker (green fluorescent protein (GFP), mCherry or Topaz) in response to cell wall breakdown (Fig. 1). If  $\beta$ -lactamase levels are too high, all the Amp is hydrolyzed, the inducer aM-Pp does not accumulate, Tet resistance is not induced, and cells are sensitive to Tet. This completes the low-pass side of a bandpass filter for protein-protein interactions.

## Results and Discussion

### The hitchhiker-bandpass circuit is externally tunable

As a test case, to determine if the hitchhiker circuit could be integrated into the bandpass circuit, we

constructed a series of hitchhiker vectors containing a set of synthetic leucine zipper coiled-coils with characterized interaction strengths [27,28] (Table 1). These sequences were originally developed using an *in vivo* dihydrofolate reductase protein fragment complementation assay and varying degrees of stringency [27]. Although hitchhiking has been demonstrated with a wide range of proteins, [18,19,22,23,29] we focused our attention on coiled-coil sequences since well-established guidelines exist for the manipulation of their binding affinities [30–32]. We used the Tat-targeting signal sequence from *E. coli* trimethylamine *N*-oxide reductase (ssTorA) and TEM-1  $\beta$ -lactamase without its native signal sequence. When cells containing a bandpass plasmid and a hitchhiker plasmid were exposed to Tet and a range of Amp concentrations, growth and fluorescence were only observed in a narrow range of Amp concentrations (Fig. 2). The Amp concentration where cell growth occurred, increased with the interaction strength of the expressed hitchhiker pair (Fig. 2a). We then tested the ability to tune the circuit using external stimuli. Increasing the concentration of IPTG is expected to increase the expression of the *tac* promoter-driven hitchhiker constructs, ultimately resulting in an increase in  $\beta$ -lactamase transport. Using the heterodimerizing hitchhiker construct WinZip A2/B1, we found that cells grew at higher concentrations of Amp in response to increasing concentrations of IPTG (Fig. 2b). Saturation of this effect was observed at approximately 500  $\mu$ M IPTG, presumably due to maximal expression levels being reached. Titrating the concentration of Tet adjusts the low-pass filter in the bandpass circuit. In the absence of Tet pressure, the low-pass filter is removed, allowing bacterial growth in low concentrations of Amp. Increasing Tet resulted in a corresponding narrowing of the band of bacterial growth (Fig. 2c).

### A mixed culture can be separated based on protein-protein interaction strength

The bandpass circuit has been used previously to separate strains based on  $\beta$ -lactamase activity levels [12,33]. In our circuit,  $\beta$ -lactamase activity levels are linked to the protein interaction strength of the hitchhiker pair, so it should therefore be possible to separate strains based on protein interaction strength. We

**Table 1.** WinZip series of hitchhiker constructs

Protein pair <sup>a</sup>	$K_D$	$T_m$ °C	Source
WinZipB1/B1	(73 $\mu$ M) <sup>b</sup>	(27.6) <sup>b</sup>	[27]
WinZipA2/A2	17 nM	54.2	[28]
WinZipA2/B1	4.5 nM	63.2	[28]

<sup>a</sup> The first protein in the pair is fused to ssTorA, and the second protein is fused to  $\beta$ -lactamase.

<sup>b</sup> Value is an estimate due to low stability of the complex [27].

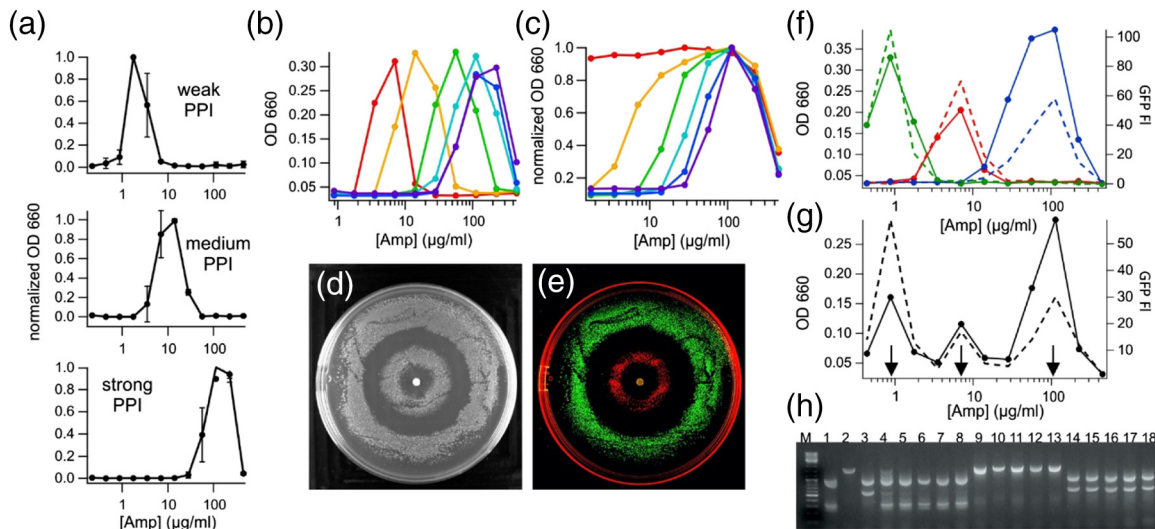


**Fig. 2.** *E. coli* with the hitchhiker-bandpass circuit only grow in a specific range of Amp concentrations that depend on the interaction strength of the expressed hitchhiker pairs and can be tuned by external stimuli. (a) Cultures with an mCherry bandpass plasmid and a hitchhiker plasmid expressing (from top to bottom) a weakly interacting hitchhiker pair (WinZip B1/B1), a medium-strength hitchhiker pair (WinZip A2/A2) or a strongly interacting pair (WinZip A2/B1) grow only in specific concentration ranges of Amp. Data show the mean OD<sub>660</sub> ( $n = 3$ ) and error bars reflect the SD. (b) Increasing the concentration of IPTG used to induce a culture expressing WinZip A2/B1 (with an mCherry bandpass plasmid) resulted in a corresponding increase in Amp required for growth. IPTG concentrations were 25 (red), 50 (yellow), 100 (green), 250 (cyan), 500 (blue) and 1000  $\mu$ M (purple). (c) Titration of the Tet concentration controls the position of the low-pass filter. The same strain described in part (b) was exposed to Tet concentrations of 0 (red), 5 (yellow), 10 (green), 15 (cyan), 20 (blue) and 25  $\mu$ M (purple). (d, e) A mixed culture of *E. coli* was separated on an agar plate containing Tet with a radial diffusion gradient of Amp. The mixed culture contained a strain with the WinZip A2/B1 hitchhiker pair and the mCherry bandpass plasmid, and a second strain with the WinZip B1/B1 hitchhiker pair and the GFP bandpass plasmid. Plating the mixed culture over the entire surface of the plate resulted in growth in two distinct rings. Fluorescence imaging (e) showed the two strains formed two separate rings of growth. (f–h) Separation of a mixed culture of three hitchhiker-bandpass strains in 96-well plate format. (f) Pure cultures of cells expressing weakly (WinZip B1/B1, green), medium (WinZip A2/A2, red) or strongly (WinZip A2/B1, blue) interacting hitchhiker pairs, containing the GFP bandpass plasmid, each grew in distinct ranges of Amp concentrations. (g) An equal mixture of these three strains produced growth maxima in three distinct ranges of Amp concentrations. The graphs show optical density (solid lines) and GFP fluorescence intensity (dashed lines). Bacteria from selected wells (indicated by arrows) were genotyped. The results are shown on an agarose gel (h). Pure cultures of each WinZip B1/B1, WinZip A2/A2 and WinZip A2/B1 (lanes 1–3, respectively) were used as controls. Lanes 4–8 show cells isolated from the low Amp well, lanes 9–13 show cells isolated from the intermediate Amp well, and lanes 14–18 show cells isolated from the high Amp well. M indicates the marker.

developed different fluorescent versions of the bandpass plasmid to create bandpass plasmids with green, red or yellow fluorescent markers (Fig. 1) so that the separation could be observed using fluorescence imaging. A mixed culture was created containing an equal mixture of cells expressing a weakly interacting hitchhiker pair (WinZip B1/B1) with the GFP bandpass plasmid, and cells expressing a strongly interacting hitchhiker pair (WinZip A2/B1) with the mCherry bandpass plasmid. The mixed culture was spread evenly on an agar plate containing IPTG, Tet, plasmid maintenance antibiotics (spectinomycin (Spec) and chloramphenicol (Cm)), and a radial diffusion gradient of Amp, created by spotting a disk of filter paper in the center of the plate with Amp. After incubation, growth appeared in two isolated rings (Fig. 2d, e). Fluorescence imaging showed the culture with the red fluorescent marker was localized in the inner ring.

These cells were expressing the strongly interacting hitchhiker pair, WinZip A2/B1, and required high levels of Amp for growth. The cells with the green fluorescent marker were expressing the weakly interacting hitchhiker pair, WinZip B1/B1, and grew where the concentration of Amp was low, forming the outer ring.

### A liquid culture format provides increased experimental control and sensitivity

Performing the hitchhiker-bandpass assay in a 96-well plate format using liquid cultures enabled a greater degree of control over the Amp gradient. First, we confirmed that cells do not obtain passive resistance due to leaked  $\beta$ -lactamase or cell wall breakdown products from neighboring cells by performing a separation of a mixed culture with two different fluorescent markers in liquid culture. The growth of

**Table 2.** cJun and cFos series of hitchhiker constructs

Hitchhiker pair <sup>a</sup>	Notes	$T_m$ (°C)	Source
cJun/cJun	Truncated leucine zippers	24	[32]
cJun(bZIP)/cJun(bZIP)	Full-length bZIP sequences	30	[34]
cFos/cJun	Truncated leucine zippers	16	[32]
cFos(bZIP)/cJun(bZIP)	Full-length bZIP sequences	50	[34]
cFos(ZIP)/cJun(bZIP)	Full-length cJun bZIP sequence, cFos leucine zipper	53	[34]

<sup>a</sup> The first protein in the pair is fused to ssTorA, and the second protein is fused to  $\beta$ -lactamase.

each strain was once again limited to a concentration range of Amp corresponding to the interaction strength of the expressed hitchhiker pairs (Figs. S2 and S3).

Precise control of the concentration of Amp in liquid cultures enabled separations of higher complexity. We separated a mixed culture of cells expressing three different WinZip peptides, with each strain co-expressing the GFP bandpass plasmid (Fig. 2f–h). The mixed culture showed growth maxima in three distinct Amp concentration ranges. Based on the Amp concentration observed to permit growth of pure cultures of each of the strains, we selected three wells from the mixed culture that were each expected to contain a pure culture after incubation. Cells were isolated by making streak plates (5 per well), and a portion of the hitchhiker plasmid was amplified by colony PCR and digested with restriction enzymes to genotype each isolated colony. Each well was found to contain a pure culture of the expected strain (Fig. 2h). This experiment was repeated three more times with genetic analysis of up to 10 isolated colonies per well. Complete separation was observed in all cases (Fig. S6).

We further analyzed the relationship between cellular Amp resistance levels and the interaction strength of the expressed protein pairs using a second series of protein–protein interactions for which extensive *in vitro* data are also available [32,34,35]. We constructed a series of hitchhiker vectors containing various lengths of the bZIP domain of cJun and cFos (Table 2). These proteins dimerize *via* a coiled-coil leucine zipper region and bind to AP-1 sites on DNA *via* a positively charged basic region. cJun can both homodimerize and heterodimerize with cFos, whereas cFos cannot form stable homodimers [36]. These constructs were tested in the hitchhiker-bandpass assay (Fig. 3). The Amp resistance levels observed correlated well with published *in vitro* data. Constructs containing truncated cJun leucine zipper homodimers and truncated cFos/cJun leucine zipper heterodimers are known to interact weakly and grew at low concentrations of Amp. The full-length cJun homodimer exhibited activity similar to the truncated version, potentially because the increase in interaction strength gained by the increased length of the cJun leucine zipper is not strong enough to offset the electrostatic repulsion of the basic domains in the full-length version. The full-length cJun/cFos heterodi-

mer constructs grew at much higher concentrations of Amp, consistent with the strong interaction strength measured *in vitro*. Removal of the cFos basic domain from the full-length construct led to growth in even higher concentrations of Amp. Removing the basic domain from one protein in a bZIP pair has been shown previously to increase the interaction strength by eliminating the electrostatic repulsion between the two positively charged basic domains [34].

### Co-expression of an inhibitor protein can modulate hitchhiker interaction strength

Although the hitchhiker circuit provides a good assessment of protein–protein interaction strength, other factors are expected to influence the cellular Amp resistance observed for a given pair. These factors include variations in the effective concentration of hitchhiker pairs, the propensity for a pair to form correct ssTorA/ $\beta$ -lactamase heterodimers (which is decreased in hitchhiker pairs with homodimerizing

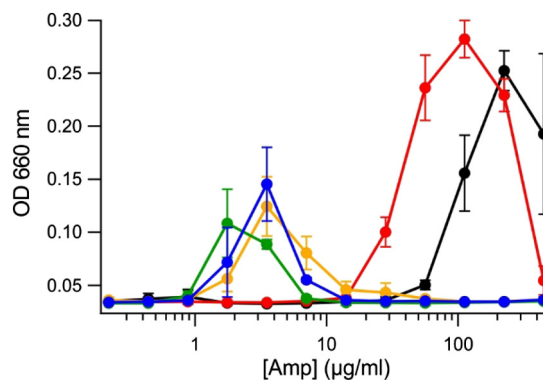


**Fig. 3.** Components of the AP-1 transcription factor were tested to compare known protein–protein interaction strength with observed cellular Amp resistance levels. Cells contained a bandpass plasmid with an mCherry marker, and a hitchhiker plasmid with one of the following protein pairs: truncated cJun/cJun (blue), cJun(bZIP)/cJun(bZIP) (yellow), truncated cFos/cJun (green), cFos(bZIP)/cJun(bZIP) (red) or cFos(ZIP)/cJun(bZIP) (black). The graph shows the mean of the optical density measurements ( $n = 3$ ), and error bars reflect the SD. Fluorescence measurements from the mCherry bandpass plasmid mirrored the optical density measurements (Fig. S7).

interaction partners), and details of how a particular pair interacts with the Tat transport machinery. The Tat export pathway has a quality control mechanism that inhibits the transport of improperly folded proteins [37]. While this feature can be beneficial, adding selection pressure for well-folded proteins [37,38], it is possible that transport efficiency may be altered by the stability of a protein–protein complex (*i.e.*, its “foldedness” at a particular temperature) in addition to the affinities of its components. To avoid any influence this may have on the selection for protein–protein interactions, we explored the option of incorporating an inhibitor of a hitchhiker protein–protein interaction to allow the binding strength of different inhibitors to be compared with respect to a single hitchhiker export pair.

Inhibitor constructs were cloned into a third compatible plasmid (Fig. 1) and were designed to contain a C-terminal fusion to blue fluorescent protein (BFP) [39] to monitor inhibitor expression levels and increase *in vivo* stability. When a strong inhibitor is co-expressed in the circuit, it is expected that it would bind to the hitchhiking protein(s) and prevent successful transport of  $\beta$ -lactamase by outcompeting the hitchhiker pair dimerization, restricting cell growth to lower concentrations of Amp. The responsiveness of the hitchhiker-bandpass assay to inhibitor strength was investigated by building and testing a series of cFos inhibitors. Previously, it was shown that potent inhibitors for bZIP proteins could be designed by appending an acidic extension to a leucine zipper, creating favorable electrostatic interactions with the basic domain of the native bZIP protein [34,40,41]. We created a series of cFos-based inhibitors containing an acidic extension of increasing length (Table 3). Co-expression of the inhibitors with the cFos(ZIP)/cJun(bZIP) hitchhiker pair shifted growth to lower concentrations of Amp in comparison to a non-inhibiting BFP-negative control (Fig. 4a). The rank order of the decrease in Amp resistance correlated with the binding strength of the inhibitors.

To confirm the ability of the hitchhiker-bandpass system to respond to inhibitors of different strength, we repeated these experiments in another protein–protein interaction system, using CREB, a bZIP transcription

factor that is analogous to cJun and cFos but functions as a homodimer. CREB hitchhiker pairs were constructed containing the CREB bZIP with an N-terminal ssTorA fusion, and the CREB leucine zipper fused to the  $\beta$ -lactamase. We created a series of inhibitors based on A4-CREB [40,42], a construct containing the CREB leucine zipper with a four-heptad repeat acidic extension, by making point mutations designed to weaken its binding (Table 4). Coiled-coil sequences form helices with a periodicity of seven residues. The residues within this heptad repeat are designated *a–g* to describe their position within the coil. Residues in the *d* positions are located along the coiled-coil interface and are typically involved in hydrophobic interactions [43,44]. We mutated two *d* position residues in the A4-CREB-BFP leucine zipper from Leu to Gly (residues L316G, L323G in the murine CREB sequence), a change that is expected to dramatically decrease stability (Table 4) [43,44]. In addition, we made a version of A4-CREB-BFP with two *f* position residues in the leucine zipper mutated to Gly (residues N318G, E325G in the murine CREB sequence). The *f* position is surface exposed, and Gly substitution at these sites is expected to have less of an effect on coiled-coil stability (Table 4) [43]. The activity of these inhibitors in the hitchhiker-bandpass assay (Fig. 4b) showed that the *d* position mutations drastically decreased the strength of the inhibitor, while the *f* position mutations had no detectable effect compared to the non-mutated A4-CREB-BFP inhibitor.

To confirm that the change in Amp resistance of the cells was due to a specific interaction between the expressed inhibitor and the hitchhiker pair, we tested the system with a non-specific inhibitor. To do so, we co-expressed the strong inhibitor A4-CREB-BFP with the cFos(ZIP)/cJun(bZIP) hitchhiker pair. This had no detectable effect on the Amp resistance of the cells in comparison to cells co-expressing a BFP-negative control with the cFos(ZIP)/cJun(bZIP) hitchhiker pair (Fig. S8).

## Summary

Protein–protein interactions *in vivo* are tuned through evolutionary pressure to optimize function; this tuning may produce weak-, intermediate- or high-affinity interactions. Currently available selection systems, however, focus on the development of interactions with high affinity, recovering all interactions above a set threshold. We have shown using well-defined test cases of known affinity that the hitchhiker-bandpass circuit allows selection pressure to be tuned to recover protein–protein interactions with affinities falling within a desired range. The ability to select for weaker or intermediate, or switchable protein–protein interaction affinity *in vivo* is expected to be useful for biotechnological applications requiring tuned interactions.

**Table 3.** Fos-based inhibitor series

Inhibitor	Notes	$T_m$ with cJun (bZIP) (°C)	Source
BFP	Negative control		
A0-Fos-BFP	Fos leucine zipper	53.4	[34]
A2-Fos-BFP	Two heptad repeats of the acidic extension	n.d.	
A4-Fos-BFP	Four heptad repeats of the acidic extension	72.1	[34]

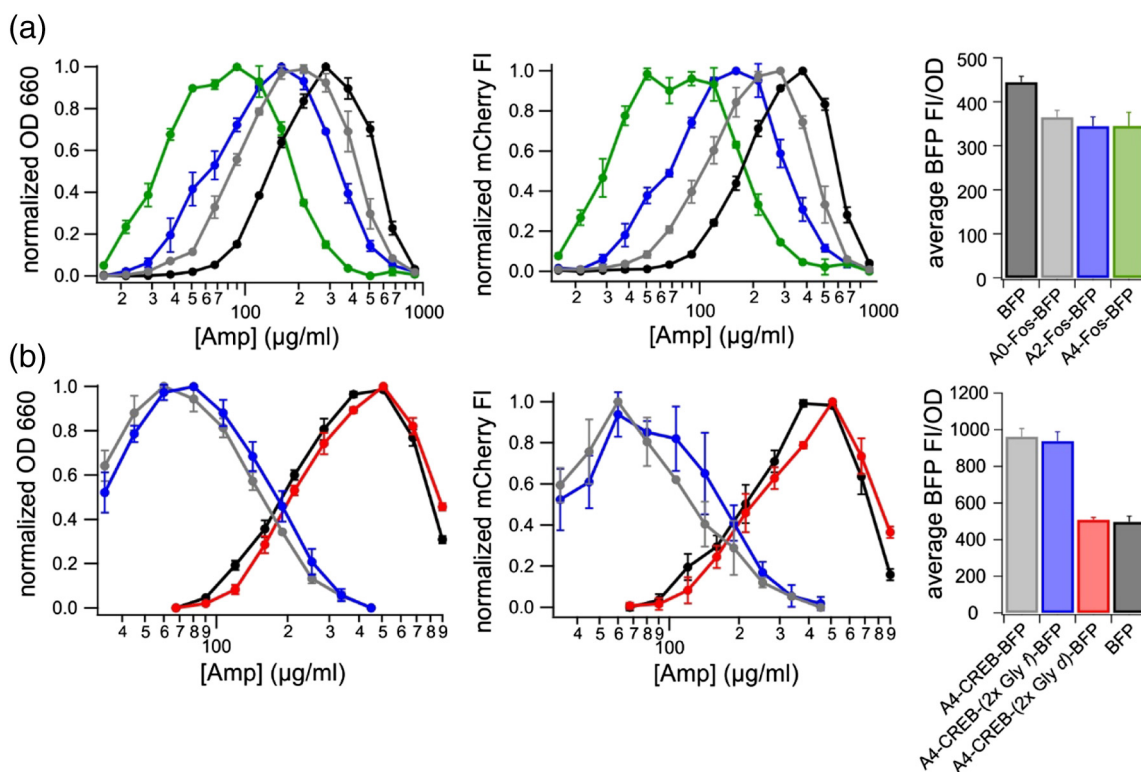


**Fig. 4.** Assessment of inhibitor strength using the hitchhiker-bandpass assay. (a) The cFos(ZIP)/cJun(bZIP) hitchhiker pair was co-expressed with a cFos-based inhibitor with an acidic extension of increasing length: BFP-negative control (black), A0-Fos-BFP (gray), A2-Fos-BFP (blue) and A4-Fos-BFP (green). (b) Assessment of CREB inhibitor strength using the hitchhiker-bandpass assay. The CREB hitchhiker pair was co-expressed with a CREB-based inhibitor: BFP-negative control (black), A4-CREB-BFP (gray), A4-CREB-BFP with two *f* positions mutated to Gly (blue) and A4-CREB-BFP with two *d* positions mutated to Gly (red). For each set, growth (OD<sub>660</sub>) (left), expression of the fluorescent mCherry reporter (middle) and inhibitor expression levels (BFP fluorescence) (right) are shown. OD and mCherry fluorescence values show the mean ( $n = 3$ ), and error bars reflect the SD. BFP fluorescence values are shown as the mean of the BFP fluorescence normalized by the OD, using data from wells that had growth (defined as an OD within 75% of the maximum OD of the culture).

## Materials and Methods

Detailed materials and methods can be found in the Supplementary Information.

### Strains

All cloning was performed using in *E. coli* XL1Blue [Stratagene, *recA1 endA1 gyrA96 thi-1 hsdR17 supE44 relA1 lac (F' proAB lacIq ZΔM15 Tn10 (Tet))*]. Hitchhiker-bandpass experiments were

performed in *E. coli* SNO301 (*ampD1, ampA1, ampC8, pyrB, recA, rpsL*) [45].

### Plasmid construction

Plasmids were constructed using classical restriction enzyme-based cloning, Gibson Assembly [46] and SLICE [47]. The bandpass plasmids were developed using pTS1 (*ClotDF13* origin of replication, Spec resistance). The hitchhiker constructs were developed using pACYCDuet2 (*p15A* origin of replication, Cm

**Table 4.** CREB-based inhibitor series

Inhibitor	Notes	$T_m$ with CREB(ZIP) (°C) <sup>a</sup>
BFP	negative control	
A4-CREB-(2x Gly f)-BFP	zipper with mutations in <i>f</i> positions (N318G, E325G)	31
A4-CREB-(2x Gly d)-BFP	zipper with mutations in <i>d</i> positions (L316G, L323G)	-2
A4-CREB-BFP	four heptad repeats of the acidic extension	34

<sup>a</sup> Prediction by bCIPA [32,35].

selectable marker). The inhibitor constructs were developed using pET24b (*ColE1/pMB1* origin of replication, Km selectable marker). The *T7* promoters in pACYCDuet2 and pET24b were exchanged with the *tac* promoter from pDIMC8-TEM-1 [12] to allow for expression in *E. coli* SNO301. Detailed plasmid information can be found in the SI.

### Culture preparations

*E. coli* SNO301 was electroporated with a bandpass plasmid, a hitchhiker plasmid and, when required, an inhibitor plasmid. A single colony was used to make an overnight culture in 5 mL of DYT (double-yeast tryptone) supplemented with Cm (25 µg/mL), Spec (100 µg/mL), (Km (50 µg/mL) for three-plasmid experiments) and 1% glucose. The following day, the culture was diluted to an OD<sub>660</sub> of 0.5 in DYT and glycerol (15% final concentration), aliquoted into 100 µL samples and stored at -80 °C.

### Agar plate experiments

Petri dishes were prepared with 15 mL of LB-agar containing Cm (25 µg/mL), Spec (100 µg/mL), Tet (20 µg/mL) and IPTG (300 µM). After solidification, plates were dried for 10 min in a laminar flow hood to decrease moisture content. A sterile disk of filter paper was placed in the center of the plate and spotted with Amp (2 µL, 100 mg/mL). The plates were left for 15 min to allow an Amp gradient to form. Glycerol stock cultures of each strain were thawed on ice, mixed in equal proportions and diluted 20-fold in DYT. The Amp disk was removed, and 150 µL of the mixed culture was spread across the entire plate and left to dry for 15 min. A second disk of filter paper was placed in the center of the plate and spotted with Amp (2 µL, 100 mg/mL). The plates were incubated for 90 min at room temperature, then at 37 °C for 20 h. After incubation, plates were stored at 4 °C for 20 h to allow for fluorescent chromophore maturation. The plates were imaged using a Fusion SL (Vilber Lourmat) imaging system with white light, and with EpiBlue LED lighting (with an F-595 Y3 filter) for the GFP marker, and EpiRed LED lighting (with an F-695 Y5 filter) for the mCherry marker. The greyscale fluorescence images were false colored, the contrast adjusted, and overlaid using ImageJ software.

### Liquid culture experiments

Round-bottom 96-well plates were prepared with 90 µL of DYT media containing Cm (25 µg/mL), Spec (100 µg/mL), (Km (50 µg/mL) for three-plasmid experiments), Tet (20 µg/mL), IPTG (500 µM) and an Amp gradient created by serial dilutions. A glycerol starter culture was thawed on ice, diluted in prepared DYT media, and 10 µL of the diluted culture was added to each well to an inoculation OD<sub>660</sub> of 0.001 for two-

plasmid experiments, 0.005 for three-plasmid experiments, and 0.007 for three-plasmid experiments co-expressing A4-CREB-BFP or A4-CREB-(2xGly f)-BFP (due to apparent toxicity of the expressed proteins). When plating a mixed culture, equal volumes of each starter culture were combined. Experiments were often performed in parallel for replicates. For Fig. 2c, the IPTG concentration used was 300 µM, and for Fig. 2f and g, the IPTG concentration was increased to 1 mM to achieve better separation of the strains. Plates were incubated with a lid at 32 °C with orbital shaking at 400 rpm for 18–20 h. Following incubation, plates were centrifuged for 15 min at 4000 rpm at 4 °C, the supernatant was removed, and cells were re-suspended in 100 µL of PBS and transferred to a flat-bottom plate for measurements. Optical density (660 nm) and fluorescence (GFP ex. 486 nm, em. 509 nm; mCherry ex. 587 nm, em. 610 nm; Topaz ex. 515 nm, em. 527 nm; BFP ex. 402 nm, em. 457 nm) were measured using an infinite M1000Pro plate reader (Tecan). In the GFP and Topaz mixed culture, GFP was excited at 466 nm to minimize background from Topaz. For the genetic analysis, streak plates were made to isolate single colonies, hitchhiker genes were amplified using colony PCR, and the amplified fragments were digested with *Pst*I and analyzed on an agarose gel.

---

### Acknowledgments

We thank Prof. Marc Ostermeier for the strain SNO301 and the plasmids pTS1-GFP and pDIMC8-TEM-1, Stefan Hoffmann for critical reading of the manuscript, and Franziska Ewert for technical assistance.

**Funding Information:** This work was supported by the National Institutes of Health (R33MH105724 to G.A.W.). K.E.B. was supported by a scholarship from the Natural Sciences and Engineering Research Council of Canada and a research grant from the German Academic Exchange Service (DAAD) Deutscher Akademischer Austauschdienst.

**Conflict of Interest Statement:** The authors declare no competing interest.

### Appendix A. Supplementary data

Supplementary data to this article can be found online at <https://doi.org/10.1016/j.jmb.2018.11.011>.

Received 24 September 2018;

Received in revised form 7 November 2018;

Accepted 8 November 2018

Available online 15 November 2018

**Keywords:**

synthetic biology;  
genetic circuit;  
biological engineering;  
protein-protein interactions;  
twin-arginine translocation;  
selection system

**Abbreviations used:**

bZIP, basic leucine zipper; Tat, twin-arginine translocation; Amp, ampicillin; aM-Pp, 1,6-anhydroMurNAc-pentapeptide; Tet, tetracycline; GFP, green fluorescent protein; BFP, blue fluorescent protein; Km, kanamycin; Spec, spectinomycin; BFP, blue fluorescent protein; Cm, chloramphenicol.

**References**

- [1] I.M. Nooren, J.M. Thornton, Diversity of protein-protein interactions, *EMBO J.* 22 (2003) 3486–3492.
- [2] A. Norris, J.D. Boeke, Silent information regulator 3: the Goldilocks of the silencing complex, *Genes Dev.* 24 (2010) 115–122.
- [3] J.E. Slansky, K.R. Jordan, The Goldilocks model for TCR-too much attraction might not be best for vaccine design, *PLoS Biol.* 8 (2010).
- [4] M. Lever, H.S. Lim, P. Kruger, J. Nguyen, N. Trendel, E. Abu-Shah, et al., Architecture of a minimal signaling pathway explains the T-cell response to a 1 million-fold variation in antigen affinity and dose, *Proc. Natl. Acad. Sci. U. S. A.* 113 (2016) E6630–E6638.
- [5] J.A. Rodriguez-Martinez, A.W. Reinke, D. Bhimsaria, A.E. Keating, A.Z. Ansari, Combinatorial bZIP dimers display complex DNA-binding specificity landscapes, *elife* 6 (2017).
- [6] J.R. Perkins, I. Diboun, B.H. Dessailly, J.G. Lees, C. Orengo, Transient protein-protein interactions: structural, functional, and network properties, *Structure* 18 (2010) 1233–1243.
- [7] G. Schreiber, A.E. Keating, Protein binding specificity versus promiscuity, *Curr. Opin. Struct. Biol.* 21 (2011) 50–61.
- [8] K. Lage, Protein-protein interactions and genetic diseases: the interactome, *Biochim. Biophys. Acta* 1842 (2014) 1971–1980.
- [9] D.P. Ryan, J.M. Matthews, Protein-protein interactions in human disease, *Curr. Opin. Struct. Biol.* 15 (2005) 441–446.
- [10] J.E. Thaxton, Z. Li, To affinity and beyond: harnessing the T cell receptor for cancer immunotherapy, *Hum. Vaccin. Immunother.* 10 (2014) 3313–3321.
- [11] M.M. Pakulska, S. Miersch, M.S. Shoichet, Designer protein delivery: from natural to engineered affinity-controlled release systems, *Science* 351 (2016) aac4750.
- [12] T. Sohka, R.A. Heins, R.M. Phelan, J.M. Greisler, C.A. Townsend, M. Ostermeier, An externally tunable bacterial band-pass filter, *Proc. Natl. Acad. Sci. U. S. A.* 106 (2009) 10135–10140.
- [13] G.P. Smith, V.A. Petrenko, Phage display, *Chem. Rev.* 97 (1997) 391–410.
- [14] J. Estojak, R. Brent, E.A. Golemis, Correlation of two-hybrid affinity data with in vitro measurements, *Mol. Cell. Biol.* 15 (1995) 5820–5829.
- [15] D. Younger, S. Berger, D. Baker, E. Klavins, High-throughput characterization of protein-protein interactions by programming yeast mating, *Proc. Natl. Acad. Sci. U. S. A.* 114 (2017) 12166–12171.
- [16] J.J. Vanantwerp, K.D. Wittrup, Fine affinity discrimination by yeast surface display and flow cytometry, *Biotechnol. Prog.* 16 (2000) 31–37.
- [17] L.L. Reich, S. Dutta, A.E. Keating, SORTCERY—a high-throughput method to affinity rank peptide ligands, *J. Mol. Biol.* 427 (2015) 2135–2150.
- [18] E.M. Strauch, G. Georgiou, A bacterial two-hybrid system based on the twin-arginine transporter pathway of *E. coli*, *Protein Sci.* 16 (2007) 1001–1008.
- [19] D. Waraho, M.P. DeLisa, Versatile selection technology for intracellular protein-protein interactions mediated by a unique bacterial hitchhiker transport mechanism, *Proc. Natl. Acad. Sci. U. S. A.* 106 (2009) 3692–3697.
- [20] G. Vadlamani, M.D. Thomas, T.R. Patel, L.J. Donald, T.M. Reeve, J. Stetefeld, et al., The beta-lactamase gene regulator AmpR is a tetramer that recognizes and binds the D-Ala-D-Ala motif of its repressor UDP-N-acetylmuramic acid (MurNAc)-pentapeptide, *J. Biol. Chem.* 290 (2015) 2630–2643.
- [21] B.C. Berks, The twin-arginine protein translocation pathway, *Annu. Rev. Biochem.* 84 (2015) 843–864.
- [22] R. Patel, S.M. Smith, C. Robinson, Protein transport by the bacterial Tat pathway, *Biochim. Biophys. Acta* 1843 (2014) 1620–1628.
- [23] A. Rodrigue, A. Chanal, K. Beck, M. Muller, L.F. Wu, Co-translocation of a periplasmic enzyme complex by a hitchhiker mechanism through the bacterial tat pathway, *J. Biol. Chem.* 274 (1999) 13223–13228.
- [24] X. Zeng, J. Lin, Beta-lactamase induction and cell wall metabolism in gram-negative bacteria, *Front. Microbiol.* 4 (2013) 128.
- [25] H. Dietz, D. Pfeifle, B. Wiedemann, The signal molecule for beta-lactamase induction in *Enterobacter cloacae* is the anhydromuramyl-pentapeptide, *Antimicrob. Agents Chemother.* 41 (1997) 2113–2120.
- [26] F. Lindberg, L. Westman, S. Normark, Regulatory components in *Citrobacter freundii* ampC beta-lactamase induction, *Proc. Natl. Acad. Sci. U. S. A.* 82 (1985) 4620–4624.
- [27] K.M. Arndt, J.N. Pelletier, K.M. Muller, T. Alber, S.W. Michnick, A. Pluckthun, A heterodimeric coiled-coil peptide pair selected in vivo from a designed library-versus-library ensemble, *J. Mol. Biol.* 295 (2000) 627–639.
- [28] K.M. Arndt, J.N. Pelletier, K.M. Muller, A. Pluckthun, T. Alber, Comparison of in vivo selection and rational design of heterodimeric coiled coils, *Structure* 10 (2002) 1235–1248.
- [29] D. Waraho-Zhmeyev, B. Meksiriporn, A.D. Portnoff, M.P. DeLisa, Optimizing recombinant antibodies for intracellular function using hitchhiker-mediated survival selection, *Protein Eng. Des. Sel.* 27 (2014) 351–358.
- [30] J.B. Kaplan, A.W. Reinke, A.E. Keating, Increasing the affinity of selective bZIP-binding peptides through surface residue redesign, *Protein Sci.* 23 (2014) 940–953.
- [31] J.M. Mason, K.M. Muller, K.M. Arndt, Considerations in the design and optimization of coiled coil structures, *Methods Mol. Biol.* 352 (2007) 35–70.
- [32] J.M. Mason, M.A. Schmitz, K.M. Muller, K.M. Arndt, Semirational design of Jun-Fos coiled coils with increased affinity: universal implications for leucine zipper prediction and design, *Proc. Natl. Acad. Sci. U. S. A.* 103 (2006) 8989–8994.
- [33] T. Sohka, R.A. Heins, M. Ostermeier, Morphogen-defined patterning of *Escherichia coli* enabled by an externally tunable band-pass filter, *J. Biol. Eng.* 3 (2009) 10.

- [34] M. Olive, D. Krylov, D.R. Echlin, K. Gardner, E. Taparowsky, C. Vinson, A dominant negative to activation protein-1 (AP1) that abolishes DNA binding and inhibits oncogenesis, *J. Biol. Chem.* 272 (1997) 18586–18594.
- [35] U.B. Hagemann, J.M. Mason, K.M. Muller, K.M. Arndt, Selection and mutational scope of peptides sequestering the Jun-Fos coiled-coil domain, *J. Mol. Biol.* 381 (2008) 73–88.
- [36] J. Hess, P. Angel, M. Schorpp-Kistner, AP-1 subunits: quarrel and harmony among siblings, *J. Cell Sci.* 117 (2004) 5965–5973.
- [37] A.C. Fisher, W. Kim, M.P. DeLisa, Genetic selection for protein solubility enabled by the folding quality control feature of the twin-arginine translocation pathway, *Protein Sci.* 15 (2006) 449–458.
- [38] J. Speck, C. Rauber, T. Kukenshoner, C. Niemoller, K.J. Mueller, P. Schleberger, et al., TAT hitchhiker selection expanded to folding helpers, multimeric interactions and combinations with protein fragment complementation, *Protein Eng. Des. Sel.* 26 (2013) 225–242.
- [39] O.M. Subach, P.J. Cranfill, M.W. Davidson, V.V. Verkhusha, An enhanced monomeric blue fluorescent protein with the high chemical stability of the chromophore, *PLoS One* 6 (2011), e28674.
- [40] S. Ahn, M. Olive, S. Aggarwal, D. Krylov, D.D. Ginty, C. Vinson, A dominant-negative inhibitor of CREB reveals that it is a general mediator of stimulus-dependent transcription of c-fos, *Mol. Cell. Biol.* 18 (1998) 967–977.
- [41] D. Krylov, M. Olive, C. Vinson, Extending dimerization interfaces: the bZIP basic region can form a coiled coil, *EMBO J.* 14 (1995) 5329–5337.
- [42] A.M. Ali, J.M. Reis, Y. Xia, A.J. Rashid, V. Mercaldo, B.J. Walters, et al., Optogenetic inhibitor of the transcription factor CREB, *Chem. Biol.* 22 (2015) 1531–1539.
- [43] J.M. Mason, K.M. Arndt, Coiled coil domains: stability, specificity, and biological implications, *Chembiochem* 5 (2004) 170–176.
- [44] J. Moitra, L. Szilak, D. Krylov, C. Vinson, Leucine is the most stabilizing aliphatic amino acid in the d position of a dimeric leucine zipper coiled coil, *Biochemistry* 36 (1997) 12567–12573.
- [45] F. Lindberg, S. Lindquist, S. Normark, Inactivation of the ampD gene causes semiconstitutive overproduction of the inducible *Citrobacter freundii* beta-lactamase, *J. Bacteriol.* 169 (1987) 1923–1928.
- [46] D.G. Gibson, L. Young, R.Y. Chuang, J.C. Venter, C.A. Hutchison III, H.O. Smith, Enzymatic assembly of DNA molecules up to several hundred kilobases, *Nat. Methods* 6 (2009) 343–345.
- [47] Y. Zhang, U. Werling, W. Edelmann, SLiCE: a novel bacterial cell extract-based DNA cloning method, *Nucleic Acids Res.* 40 (2012) e55.